Detoxification

DOI: 10.1002/anie.201310123

Magnetic Titanium Dioxide Nanocomposites for Surface-Enhanced Resonance Raman Spectroscopic Determination and Degradation of Toxic Anilines and Phenols**

Xiao Xia Han, Lei Chen, Uwe Kuhlmann, Claudia Schulz, Inez M. Weidinger, and Peter Hildebrandt**

Abstract: *Mesoporous M-TiO_2 NCs, functionalized by PATP, can capture toxic anilines and phenols by azo coupling. Loading these nanodevices with Ag NPs offers the possibility for a sensitive quantitative determination of target compounds by SERRS spectroscopy, which allows multiplex detection because of the specific vibrational fingerprints. Sensitivity and selectivity can be further enhanced by concentrating the hybrid particles by an external magnet and compound-specific binding (anilines versus phenols). The bound toxic compounds can be degraded by TiO_2-assisted photocatalysis after removal of the loaded hybrid particles from the sample solution with an external magnet. The degradation process can be enhanced in the presence of plasmonic Ag nanostructures.*

Benzidine and its derivatives may metabolize to carcinogenic amines in human bodies, and thus increasing attention is paid on the potential risk (for example, bladder cancer) of human exposure to commercial products containing benzidine and its congener-based dyes.[1,2] Some phenol derivatives, widely employed in manufacturing daily used products, are hormone-like endocrine disruptors, and potentially increase risks for breast cancer.[3,4] Herein we designed multifunctional nanocomposites that allow highly sensitive detection, manipulation, and photodegradation of toxic benzidine and phenol derivatives. Magnetic TiO_2 nanocomposites (M-TiO_2 NCs) were synthesized and functionalized with *p*-aminothiophenol (PATP) for capturing target molecules by azo coupling. Owing to the specific surface-enhanced resonance Raman scattering (SERRS) fingerprints of the azo products, it was possible to identify toxic target anilines and phenols. Furthermore, azo compound degradation and nanomaterial recycling was achieved by TiO_2-assisted and plasmon-enhanced photocatalysis.

Conventional detection methods for anilines and phenols are liquid or gas chromatography combined with mass spectrometry.[5,6] Immunochemical-, fluorescence-, or aptamer-based analytical approaches have also been recently developed.[7,8] However, none of these methods combines high sensitivity with the ability of easy manipulation and detoxification.

The property of directed translocation of substrates constitutes a wide range of applications of magnetic NPs in catalysis, biological separation, and biomedicine.[9,10] Photocatalytic degradation of toxic dyes can be achieved by TiO_2 supports.[11] TiO_2 is a non-toxic and biocompatible material with unique optical and photocatalytic properties, which is used in various applications such as solar cells, waste water treatments, and drug delivery.[12] Especially intriguing is the idea to combine nanoparticles (NPs) of different functionalities in metal, metal oxide, or semiconductor NCs to exploit simultaneously analyte binding, optical, catalytic, or magnetic properties, such as Fe_3O_4/Ag or Fe_3O_4/TiO_2 hybrid NPs.[13–15]

Additional functionality may be achieved if such dual magnetic NCs also allow multiplex detection of the toxic targets by in situ spectroscopy. In this respect, SE(R)RS spectroscopy has a great potential,[16,17] such as for determining toxic metal ions, H_2O_2, and small organic molecules in water, food, and environmental safety assessment.[18–21] Moreover, introducing plasmonic materials required for SERS spectroscopy may also enhance surface-confined photochemical activity.[22] The concept of this work is depicted in Scheme 1.

Fe_3O_4 NPs, synthesized by a solvothermal reaction,[23] are of spherical shape with an average diameter of 200 nm (Figure S1 A,D; Supporting Information). TiO_2 coating was performed by hydrolysis of tetrabutylorthotitanate (TBOT), leading to a well-defined core-shell structure (Figure S1 B).

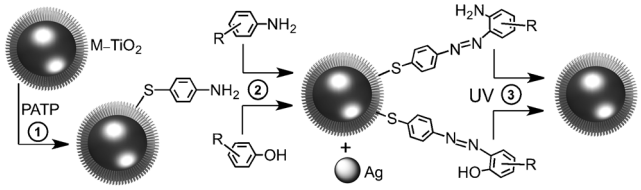

Scheme 1. 1) Functionalization of magnetic TiO_2 NPs with PATP, 2) azo coupling reaction and SERRS-based detection, and 3) UV-induced degradation.

[*] Dr. X. X. Han, Dr. U. Kuhlmann, C. Schulz, Prof. I. M. Weidinger, Prof. P. Hildebrandt
Institut für Chemie, Technische Universität Berlin
Sekr. PC14, Strasse des 17. Juni 135, 10623 Berlin (Germany)
E-mail: i.weidinger@mailbox.tu-berlin.de
hildebrandt@chem.tu-berlin.de

Dr. L. Chen
State Key Laboratory of Supramolecular Structure and Materials
Jilin University
2699 Qianjin Street, Changchun 130012 (P.R. China)

[**] The work was supported by the DFG (Cluster of Excellence UniCat; I.M.W., P.H.), and the Senate of Berlin ("Nachhaltige Chemie") (P.H.). X.X.H. acknowledges a fellowship from the Alexander-von-Humboldt Foundation.

Supporting information for this article is available on the WWW under http://dx.doi.org/10.1002/anie.201310123.

The compact TiO_2 shells changed to mesoporous structure during a hydrothermal process (Figure S1 C,E). Thus, in these nanocomposites (M-TiO_2 NCs), the surface area of TiO_2 is increased,[14] which is advantageous for PATP loading.

The initial black Fe_3O_4 suspension changed to brown after hydrothermal treatment (Supporting Information, inset in Figure S2). The TiO_2 shells and their crystalline phase were confirmed by X-ray diffraction (XRD). Besides the Fe_3O_4 XRD peaks (Figure S2 a), additional bands at 25.5, 38.1, and 48.2° that are due to anatase TiO_2 (symbol A) were observed (Figure S2 b).[14] Moreover, the M-TiO_2 NCs could be rapidly collected by an external magnet (inset in Figure S2) within 1 min, indicating preservation of the magnetic responsivity of the Fe_3O_4 NPs after TiO_2 coating.

PATP can covalently bind to TiO_2 by SH functional groups.[24] In fact, a weak Raman spectrum of PATP bound to M-TiO_2 NCs could be detected (Figure 1 B). Upon addition of

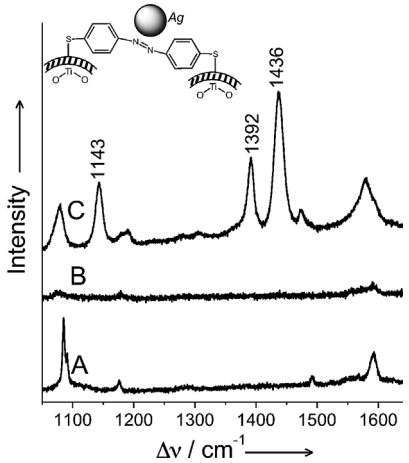

Figure 1. A) Raman spectrum of PATP powder, B) (SE)RS spectrum of PATP-functionalized M-TiO_2 NCs (20 μL), and C) SERRS spectrum of PATP-functionalized M-TiO_2 NCs (20 μL) with Ag NPs (20 μL).

Ag NPs, distinctly stronger bands were observed that are due to the SERS enhancement provided by the plasmonic Ag NPs. As reported previously, on Ag substrates, PATP could be oxidized to form 4,4′-dimercaptoazobenzene (DMAB) during SERS measurements due to a laser-induced surface reaction.[25] We also observed SERRS bands of DMAB at 1143, 1392 and 1436 cm^{-1} in the SERRS spectrum of PATP at the M-TiO_2 and Ag interfaces (Figure 1 C), thereby confirming the successful attachment of PATP at the M-TiO_2 NCs.

Herein, two anilines, namely benzidine (BD) and 2-naphthylamine (NA), and two phenols, namely bisphenol A (BPA) and nonylphenol (NPH), were used as target molecules (Figure 3). Diazonium salts obtained by HCl and $NaNO_2$ at low temperature can react with both anilines and phenols (Supporting Information, Figure S3 A). Phenols are activated in alkaline solution to form phenoxide prior to azo coupling, while anilines form azo compounds in neutral or weakly acidic solutions.[26] Thus, in mixed samples, anilines and phenols can be selectively coupled to PATP depending on the pH. Furthermore, in contrast to diazonium ions, the azo products are stable at room temperature, which is essential for SERRS measurements.

With decreasing target molecule concentration, the SERRS intensities become weaker and are eventually obscured by the background signals of the sample. However, the adsorbed azo products on the M-TiO_2 NCs can be separated from the bulk solution by a magnet to concentrate the target molecules for SERRS measurements, thereby largely eliminating spectral contributions from other compounds. For all of the SERRS measurements, we employed the 413 nm excitation line, which affords optimum surface enhancement for the Ag NPs used in this work, and provides comparably strong molecular resonance enhancement for the four azo compounds, which all show electronic transitions around this wavelength (Supporting Information, Figure S4). The diazonium ions that did not react with target molecules were unstable at room temperature, resulting in the formation of *p*-mercaptophenol[28] (Supporting Information, Figure S3 B), which, due to weak affinity of the phenol group to Ag NPs,[27] was almost undetectable by SERS spectroscopy and thus did not interfere with the SERRS analysis of the azo compounds (Supporting Information, Figure S6).

Recently, a weak enhancement of Raman scattering was reported for TiO_2 nanomaterials, which is however much lower than that of Ag nanostructures.[28,29] In fact, weak (SE)RRS bands of the azo compound on M-TiO_2 NCs were observed (Figure 2). To increase the sensitivity of the

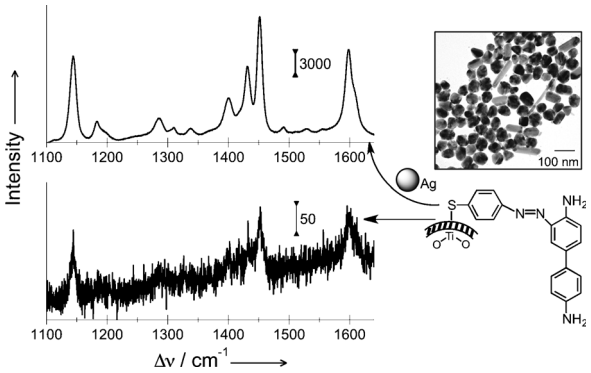

Figure 2. SERRS spectra of BD-derived azo compounds (1 ppm BD) on the M-TiO_2 NCs with (top) and without (bottom) Ag NPs. The molecular structure of the BD-derived azo compound and a TEM image of the Ag NPs are shown on the right side.

spectroscopic approach, the M-TiO_2-Azo NCs were mixed with Ag NPs before Raman measurements. A magnet was fixed under the M-TiO_2 samples during all Raman measurements. As expected, the SERRS intensity increased at least by a factor of 100 in the presence of Ag NPs[30] (Figure 2), which is due to the electromagnetic field enhancement by the plasmonic Ag NPs.

SERRS spectra of the azo products of the four target molecules in the presence of Ag NPs display unique fingerprints for each compound, demonstrating that identification of the individual anilines and phenols is possible (Figure 3).

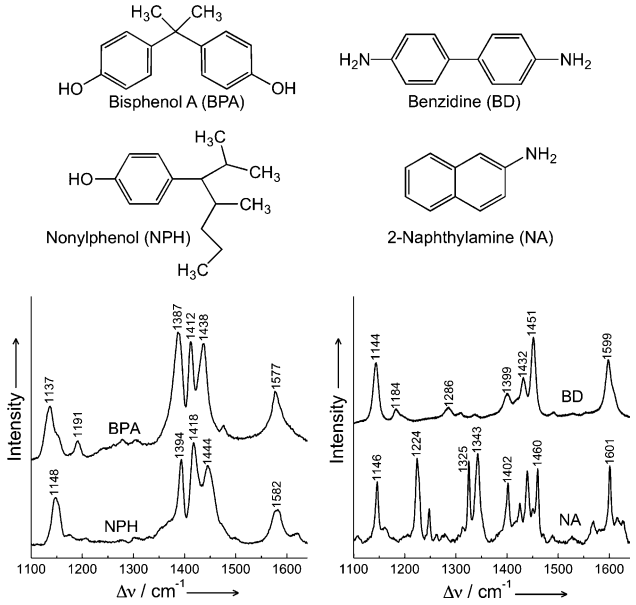

Figure 3. Structures of the target molecules and SERRS spectra of the azo products from BPA, NPH, BD, and NA (1 ppm) adsorbed on M-TiO_2 NCs upon addition of Ag NPs. During the SERRS experiments, the samples were continuously moved through the exciting laser beam.

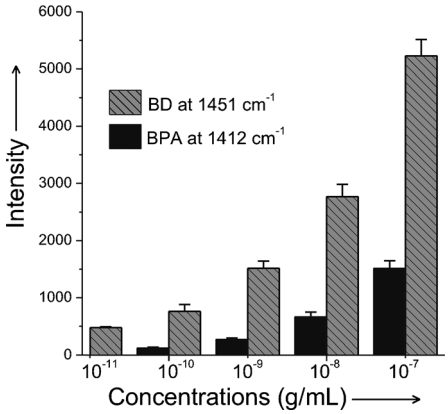

Figure 4. Concentration-dependent SERRS intensities of the azo compounds of BD and BPA. Error bars represent the standard deviations for three batches.

These characteristic vibrational signatures as well as the pH-dependent capture of either anilines and/or phenols allow for the specific detection of each compound in a mixture (Supporting Information, Figure S5).

The limit of detection (LOD) was found to be as low as 0.1 ppb for BPA and 0.01 ppb for BD (Figure 4; Supporting Information, Figure S6). These values are lower by a factor of 500 (BPA) and 300 (BD) than the reference dose for chronic oral exposure of U.S. Environmental Protection Agency. Furthermore, the present approach displays LODs comparable to the lowest LODs for BD and BPA.[7,31]

Azo compounds can be degraded by TiO_2-assisted photocatalysis upon UV-light irradiation.[11] To check the photodegradation capability of the present M-TiO_2 devices, azo products from PATP and BD were mixed with M-TiO_2 NCs and exposed to UV irradiation (312 nm). Here, free PATP was used since for PATP-attached M-TiO_2 NCs, the azo compounds could hardly be detected by the UV/Vis spectra owing to the high background and the limited concentrations of the PATP azo-derivatives on the M-TiO_2 NCs. After UV irradiation, the M-TiO_2 NCs were separated by a magnet and the supernatants were monitored by UV/Vis spectroscopy. The lack of characteristic absorption bands of the BD-derived azo compounds at 280 and 430 nm after 2 h UV irradiation indicates the decomposition of the azo products (Figure 5). After UV-assisted self-cleaning, the M-TiO_2 NCs can be re-used for PATP functionalization and subsequent determination of target molecules. In fact, spectra of PATP re-attached to M-TiO_2 NCs (Supporting Information, Figure S7) are very similar to those in Figure 1. Thus, the photocatalytic property of TiO_2 shells allows for azo product degradation as well as for nanomaterial recycling.

Furthermore, we investigated the effect of plasmon enhancement of the TiO_2-assisted photodegradation. Here the 413 nm laser line was used for both photodegradation and SERRS spectroscopy. To achieve plasmon-induced surface enhancement at the TiO_2/azo interface, a magnet was fixed

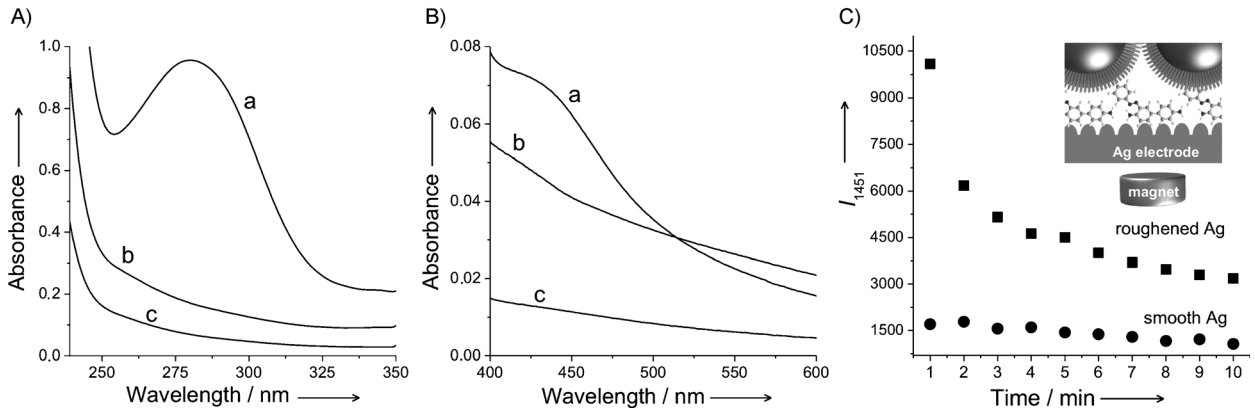

Figure 5. A) UV/Vis spectra of BD (1 mg mL^{-1})-derived azo product without M-TiO_2 NCs (a), and mixed with M-TiO_2 NCs after exposure to UV irradiation for b) 1 h and c) 2 h; C) SERRS band intensities at 1451 cm^{-1} of BD ($\delta = 10$ ppm)-derived azo products at the interfaces of the M-TiO_2 NCs and Ag electrodes as a function of laser exposure time.

under an electrochemically roughened or a smooth Ag support (inset of Figure 5C) exposed to an M-TiO_2-azo NC containing solution. The M-TiO_2-azo NCs were then magnetically collected on the respective Ag surface. SERRS spectra of azo products were detectable on both TiO_2/Ag interfaces, albeit with different intensity (Supporting Information, Figure S8). The stronger SERRS spectra on rough Ag supports are attributed to the much higher plasmonic field enhancement owing to the nanostructured Ag surface.[32]

Noble metals, such as Ag and Au, can act as an electron trap and promote interfacial charge transfer processes at the TiO_2 interface, which may improve the photocatalytic efficiency of TiO_2.[33] However, only when the M-TiO_2-azo NCs are brought in close contact to the roughened Ag surface, the photodegradation efficiency is increased, which is presumably due to the electric field enhancement at the TiO_2/azo interface (Figure 5C). In the case of rough Ag supports, the SERRS intensity at 1451 cm^{-1} decreased sharply during the first 2 min, eventually leading to a 70% decrease after 10 min exposure to the laser beam. Under otherwise identical conditions the decrease was only 35% for smooth Ag supports. The faster intensity decay at the rough Ag electrode confirms the plasmonic field enhancement of the photodegradation.

In summary, mesoporous M-TiO_2 NCs, functionalized by PATP, can capture toxic anilines and phenols by azo coupling. Loading these nanodevices with Ag NPs offers the possibility for a sensitive quantitative determination of target compounds by SERRS spectroscopy, which allows multiplex detection by the specific vibrational fingerprints. Sensitivity and selectivity can be further enhanced by concentrating the hybrid particles by an external magnet and compound-specific binding (anilines versus phenols). Apart from the analytical power, the bound toxic compounds can be degraded via TiO_2-assisted photocatalysis in situ or ex situ after removal of the loaded hybrid particles from the sample solution by an external magnet. The degradation process can also be enhanced in the presence of plasmonic Ag nanostructures. Thus, M-TiO_2 NCs represent promising devices for toxicity assessment and elimination in practical applications for safety assessment of food, environment, and commercial products.

Received: November 21, 2013
Published online: January 28, 2014

Keywords: aniline · magnetic TiO_2 · phenol · photocatalysis · SERRS

[1] G. P. Hemstreet, S. Yin, Z. Ma, R. B. Bonner, W. Bi, J. Y. Rao, M. Zang, Q. Zheng, B. Bane, N. Asal, G. Li, P. Feng, R. E. Hurst, W. Wang, *J. Natl. Cancer Inst.* **2001**, *93*, 427 – 436.
[2] N. Rothman, R. B. Hayes, T. V. Zenser, D. M. DeMarini, W. Bi, A. Hirvonen, G. Talaska, V. K. Bhatnagar, N. E. Caporaso, L. R. Brooks, V. M. Lakshmi, P. Feng, S. K. Kashyap, X. You, B. T. Eischen, R. Kashyap, M. L. Shelton, F. F. Hsu, M. Jaeger, D. J. Parikh, B. B. Davis, S. Yin, D. A. Bell, *Cancer Epidemiol. Biomarkers Prev.* **1996**, *5*, 979 – 983.
[3] L. N. Vandenberg, M. V. Maffini, C. Sonnenschein, B. S. Rubin, A. M. Soto, *Endocr. Rev.* **2009**, *30*, 75 – 95.
[4] K. W. Lozada, R. A. Keri, *Biol. Reprod.* **2011**, *85*, 490 – 497.
[5] L. E. Vera-Avila, A. Garcia-Ac, R. Covarrubias-Herrera, *J. Chromatogr. Sci.* **2001**, *39*, 301 – 307.
[6] E. Ferrer, E. Santoni, S. Vittori, G. Font, J. Manes, G. Sagratini, *Food Chem.* **2011**, *126*, 360 – 367.
[7] Z. Chen, G. Zhang, X. Chen, Y. Peng, Y. Lin, S. Lu, *Anal. Methods* **2011**, *3*, 1845 – 1850.
[8] B. Kang, J. H. Kim, S. Kim, K. H. Yoo, *Appl. Phys. Lett.* **2011**, *98*, 073703.
[9] J. Gao, H. Gu, B. Xu, *Acc. Chem. Res.* **2009**, *42*, 1097 – 1107.
[10] J. Liu, S. Z. Qiao, Q. H. Hu, G. Q. Lu, *Small* **2011**, *7*, 425 – 443.
[11] I. K. Konstantinou, T. A. Albanis, *Appl. Catal. B* **2004**, *49*, 1 – 14.
[12] P. Roy, S. Berger, P. Schmuki, *Angew. Chem.* **2011**, *123*, 2956 – 2995; *Angew. Chem. Int. Ed.* **2011**, *50*, 2904 – 2939.
[13] C. S. Levin, C. Hofmann, T. A. Ali, A. T. Kelly, E. Morosan, P. Nordlander, K. H. Whitmire, N. J. Halas, *ACS Nano* **2009**, *3*, 1379 – 1388.
[14] W. F. Ma, Y. Zhang, L. L. Li, L. J. You, P. Zhang, Y. T. Zhang, J. M. Li, M. Yu, J. Guo, H. J. Lu, C. C. Wang, *ACS Nano* **2012**, *6*, 3179 – 3188.
[15] R. Chalasani, S. Vasudevan, *ACS Nano* **2013**, *7*, 4093 – 4104.
[16] K. Kneipp, M. Moskovits, H. Kneipp, *Surface-Enhanced Raman Scattering*: *Physics and Applications*, Springer, Berlin, **2006**.
[17] D. H. Murgida, P. Hildebrandt, *Chem. Soc. Rev.* **2008**, *37*, 937 – 945.
[18] V. M. Zamarion, R. A. Timm, K. Araki, H. E. Toma, *Inorg. Chem.* **2008**, *47*, 2934 – 2936.
[19] S. S. R. Dasary, A. K. Singh, D. Senapati, H. Yu, P. C. Ray, *J. Am. Chem. Soc.* **2009**, *131*, 13806 – 13812.
[20] X. X. Han, Y. Ozaki, B. Zhao, *TrAC Trends Anal. Chem.* **2012**, *38*, 67 – 78.
[21] X. X. Han, A. M. Schmidt, G. Marten, A. Fischer, I. M. Weidinger, P. Hildebrandt, *ACS Nano* **2013**, *7*, 3212 – 3220.
[22] S. Linic, P. Christopher, D. B. Ingram, *Nat. Mater.* **2011**, *10*, 911 – 921.
[23] Y. Deng, D. Qi, C. Deng, X. Zhang, D. Zhao, *J. Am. Chem. Soc.* **2008**, *130*, 28 – 29.
[24] L. Yang, X. Jiang, W. Ruan, B. Zhao, W. Xu, J. R. Lombardi, *J. Phys. Chem. C* **2008**, *112*, 20095 – 20098.
[25] Y.-F. Huang, H.-P. Zhu, G.-K. Liu, D.-Y. Wu, B. Ren, Z.-Q. Tian, *J. Am. Chem. Soc.* **2010**, *132*, 9244 – 9246.
[26] R. M. Christie, *Color Chemistry*, Royal Society of Chemistry, Cambridge, **2001**.
[27] X. X. Han, P. Pienpinijtham, B. Zhao, Y. Ozaki, *Anal. Chem.* **2011**, *83*, 8582 – 8588.
[28] I. Alessandri, *J. Am. Chem. Soc.* **2013**, *135*, 5541 – 5544.
[29] X. X. Han, C. Köhler, J. Kozuch, U. Kuhlmann, L. Paasche, A. Sivanesan, I. M. Weidinger, P. Hildebrandt, *Small* **2013**, *9*, 4175 – 4181.
[30] P. C. Lee, D. Meisel, *J. Phys. Chem.* **1982**, *86*, 3391 – 3395.
[31] K. Hegnerová, M. Piliarik, M. Steinbachová, Z. Flegelová, H. Cernohorská, J. Homola, *Anal. Bioanal. Chem.* **2010**, *398*, 1963 – 1966.
[32] A. Sivanesan, K. H. Ly, W. Adamkiewicz, K. Stiba, S. Leimkühler, I. M. Weidinger, *J. Phys. Chem. C* **2013**, *117*, 11866 – 11872.
[33] M. M. Khan, S. A. Ansari, M. I. Amal, J. Lee, M. H. Cho, *Nanoscale* **2013**, *5*, 4427 – 4435.

